JOURNAL OF MATERIALS SCIENCE 20 (1985) 255–260

Thermal degradation behaviour of montmorillonite – α-naphthylamine complex under nitrogen

A. ŌYA, Y. OMATA, S. ŌTANI
Faculty of Engineering, Gunma University, Kiryu, Gunma 376, Japan

A thin film of montmorillonite–α-naphthylamine complex (MNC) was prepared, and then subjected to γ-ray radiation and heating to 473 K for polymerization of the inserted naphthylamine. MNC was subsequently heated to various temperatures below 1473 K under nitrogen. Montmorillonite film (Mont) was also treated in the same way as the reference sample. Compared with Mont, the MNC-layered structure was remarkably thermally stable and remained so slightly, even after heating to 1273 K. MNC was found to have a homogeneous porous structure after heating to 1273 K. Through comparison with Mont, the thermal degradation behaviour of MNC is discussed on the basis of X-ray diffraction, FT-IR, TG-DTA, elemental analysis, mass spectrum and SEM observations.

1. Introduction

Layered compounds and their complexes have been widely studied to develop functional materials such as catalysts, superconductors and so on [1, 2]. We were interested in preparing new types of functional materials through heat-treating the layer-type complexes consisting of layered inorganic and organic compounds. In order to obtain fundamental data for this attempt, the thermal degradation behaviour of the layer-type complexes of TaS_2–α-naphthylamine [3] and FeOCl–organic compounds [4] have been studied previously.

Montmorillonite is a typical layered inorganic compound forming the layer-type complexes with organic compounds. There are many works on this subject [5, 6], but just few papers describe the thermal behaviour of the complexes under heating to not such a high temperature [7–9]. There is no work on the development of new functional materials through thermal degradation of the complexes. We have reported briefly that the layered structure of the montmorillonite–α-naphthylamine complex has a higher thermal stability under nitrogen than montmorillonite itself [10]. In the present work, the thermal degradation behaviour of this complex was revealed in more detail through comparison with that of montmorillonite.

2. Experimental details

2.1. Preparation procedures of samples

Crude montmorillonite from Aterasawa, Yamagata, Japan, was kindly supplied by Kunimine Ind Co. Fractions smaller than 2 μm were corrected by sedimentation. Its chemical formula is

$$M(Al_{3.40}Fe^{3+}_{0.09}Fe^{2+}_{0.06}Mg_{0.47})(Si_{7.65}Al_{0.35})O_{20}(OH)_4 \cdot nH_2O,$$

where M is alkali metal. After converting to the lithium form, the self-supporting film less than several tens of microns thickness was prepared according to the procedure described elsewhere [11].

1 g of the self-supporting film of montmorillonite was soaked in 300 ml 0.1 N naphthylamine · hydrochloride (NA) aqueous solution at 353 K for 3 days to convert into montmorillonite–α-naphthylamine complex film (abbreviation: MNC). MNC was washed with acetone to remove NA on the film surface and then dried. Next MNC was sealed in the pyrex glass tubing under vacuum, followed by γ-ray radiation of 12 Mrad and heat-treatment to 473 K for 1 h in order to polymerize the inserted NA more effectively. The radiated MNC was finally heated to temperatures between 673 and 1473 K at a heating rate of 5 K min^{-1}

0022–2461/85 \$03.00 + .12

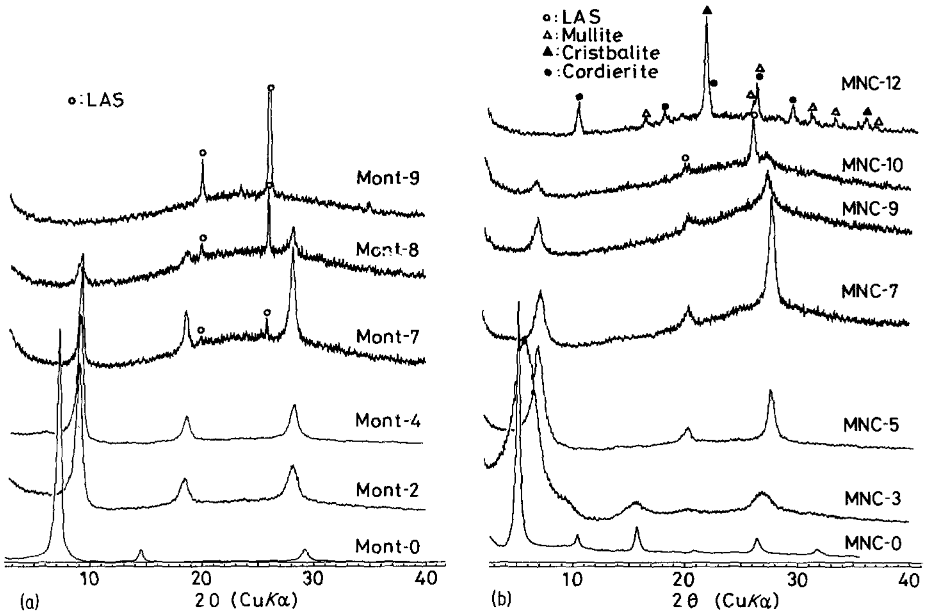

Figure 1 Changes of X-ray diffraction profiles of (a) Mont and (b) MNC with HTT.

and kept for 1 h under nitrogen. Mont was also treated by same procedures as a reference. In this paper, samples are labelled by appending the heat-treatment temperature ($\times 10^{-2}$ °C) after Mont and MNC, e.g. MNC-0 and Mont-10 are raw MNC with no further treatment and Mont heated to 1273 K (1000° C), respectively.

2.2. Measurements

The Ni-filtered Cu$K\alpha$ radiation was used for X-ray diffraction analysis. FT-IR was measured in a KBr pellet. The fracture surface of the film was observed using scanning electron microscopy (SEM). MNC-2 and Mont-2 were subjected to thermogravimetry at a heating rate of 5 K min^{-1} in a stream of nitrogen. MNC-2 and MNC-6 were sealed in the quartz glass tubing under vacuum and then heated to 873 and 1473 K, respectively. The gases evolved during these processes were identified using mass spectrometry.

3. Results

3.1. X-ray diffraction

Figs. 1a and b show changes in the X-ray diffraction profiles of Mont and MNC with heat-treatment temperature (HTT). Their basal spacings, d_{001}, are summarized in Table I. Mont-0, of which d_{001} is 1.23 nm, exhibited an X-ray diffraction profile with sharp peaks. This d_{001} decreased remarkably to 0.97 nm through dehydration during γ-ray radiation and subsequent heating to 473 K, and then remained unchanged up to 1073 K (Mont-8). The crystal lattice of Mont was completely destroyed at 1173 K (Mont-9). A lithium aluminium silicate crystal (LAS) appeared weakly at 973 K (Mont-7) and strengthened its diffraction intensities with increase in HTT [12].

On the other hand, d_{001} of MNC-0 is 1.70 nm which is larger than that of the dehydrated Mont by 0.74 nm, and decreased gradually to 1.26 nm of MNC-4 with an increase in HTT. Just a small change was observed in d_{001} at higher HTT to 1273 K (MNC-10), although its diffraction intensities decreased gradually. The (1 0 1) peak of the LAS crystal appeared in MNC-10 and changed into

TABLE I Basal spacings of MNC and Mont with HTT

HTT		Basal spacing (nm)	
(K)	(° C)	MNC	Mont
No-heating		1.70	1.23
473	200	1.68	0.97
573	300	1.52	0.97
673	400	1.26	0.96
773	500	1.28	0.95
873	600	1.28	0.95
973	700	1.24	0.95
1073	800	1.26	0.95
1173	900	1.28	*
1273	1000	1.30	*
1473	1200	*	–

*The layer structure was destroyed.

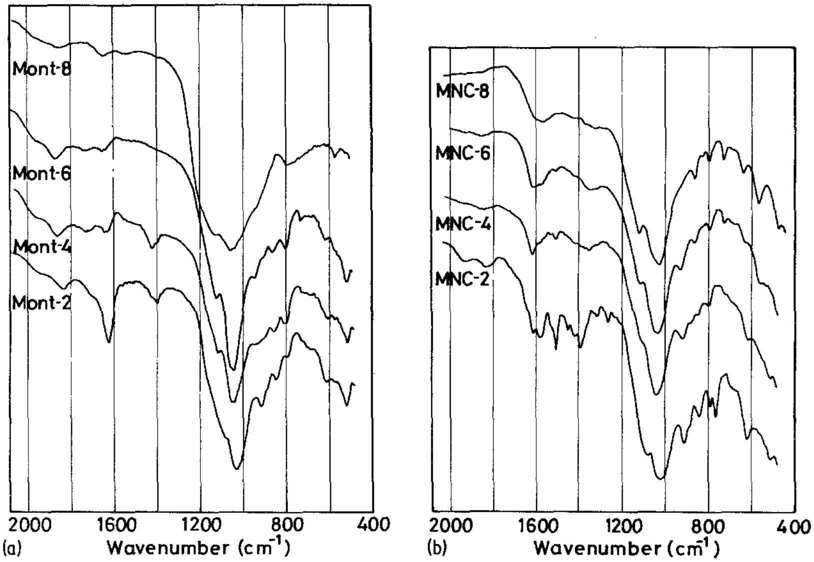

Figure 2 FT-IR spectra of (a) Mont and (b) MNC after heating.

mullite, cristobalite and cordierite at 1473 K (MNC-12). Crystal phases derived from MNC and Mont at high HTT will be described in more detail later.

3.2. FT-IR spectroscopy

Figs. 2a and b show FT-IR spectra of Mont and MNC after heating to 473 to 1073 K. In the spectrum of Mont-2, as is well known, the two peaks at 1037 and 1088 cm^{-1} are assigned to Si–O stretching, and other peaks are all characteristic of montmorillonite, although their assignments are not necessarily clear [13–14]. A peak at 1620 cm^{-1} is attributable to hydroxy-OH. In Mont-4 and Mont-6 the peak at 1620 cm^{-1} disappeared, as did the peak at 1423 cm^{-1} in Mont-6. Compared with these spectra, the spectrum of Mont-8 is not clear, especially between 800 and 1200 cm^{-1} possibly assigning to Si–O and Al–O [14].

MNC-2 exhibited peaks at 1560 cm^{-1} from NH_2, 1400 to 1500 cm^{-1} and 750 to 800 cm^{-1} from aromatic C–H and 1280 cm^{-1} from C_{arom}–N, in addition to those observed in Mont-2. These peaks, however, disappeared in MNC-4, except for a small peak at 1500 cm^{-1}, which eventually disappeared in MNC-6. It should be noted that even in MNC-8, some peaks between 500 and 900 cm^{-1} were clearly observed.

3.3. Thermogravimetry

Fig. 3 shows TG-DTA curves of Mont-2 and MNC-2 in a stream of nitrogen. Mont-2 exhibited a weight decrease accompanied by an endothermic peak around 300 to 450 K, which is attributable to removal of absorped water. The next weight decrease begins just below 900 K by dehydroxylation. Whereas, MNC-2 exhibited a weight decrease with a weak exothermic peak at 500 to 850 K, the decrease reached 25% at 1400 K.

3.4. Elemental analysis

Elemental analyses of Mont and MNC are summarized in Table II. Organic compounds between inorganic compound layers are usually difficult to burn off completely in the elemental analysis apparatus, so that some error is unavoidable. Just small variations with HTT were observed in the analytical data of Mont in Table II, which may exhibit the accuracy of this technique. The carbon, hydrogen and nitrogen content in MNC, on the other hand, decreased on heating to 773 K (MNC-5), quite remarkably between 573 and

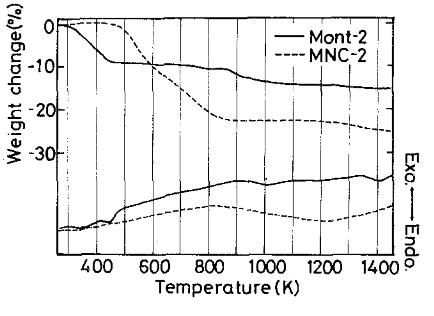

Figure 3 TG-DTA curves of Mont-2 and MNC-2 in nitrogen.

TABLE II Elemental analyses of MNC and Mont with HTT (wt%)

HTT		MNC			Mont		
(K)	(°C)	C	H	N	C	H	N
No-heating		15.7	2.0	2.4	0.3	0.7	0.7
473	200	11.9	1.7	2.9	0.4	0.6	0.6
573	300	9.6	1.5	1.3	–	–	–
673	400	3.2	1.2	1.3	0.3	0.5	0.7
773	500	1.3	0.6	0.9	0.3	0.4	0.6
873	600	1.2	0.4	0.9	–	–	–
973	700	0.8	0.3	0.8	0.3	0.1	0.9
1073	800	0.6	0.1	0.5	0.2	0.0	0.6
1173	900	0.8	0.0	1.5	0.3	0.0	0.5
1273	1000	0.6	0.1	0.0	–	–	–
1473	1200	1.6	0.1	0.0	–	–	–

673 K. The carbon content remained unchanged at higher HTT up to 1273 K and then increased slightly again at 1473 K.

3.5. Mass spectrometry

Identification of gases evolved from MNC are shown in Table III. H_2O and/or NH_3 are the main gases evolved during heating to between 473 and 873 K. Aniline was also observed. At higher HTT (873 to 1473 K) CO and CO_2 were evolved unsteadily mainly from MNC.

3.6. SEM observation

Figs. 4a and b are SEM photographs of the fracture surfaces of Mont and MNC before and after heating. Mont-0, being a slightly thicker film, consists of rough stacking of the layers. Such a layer stacking seems to become more dense in Mont-4. Here in the seriously curved layer stacking can also be seen. The densely sintered film surfaces of Mont-8 were separated: the film surface was possibly sintered normally and then separated by gases evolved within the film at higher HTT. The film seems to have passed through a fusion stage, in view of the formation of needle-like products (arrowed). The fusion state of Mont-10 must be more serious, because the needle-like products and the pores are more rounded.

MNC-0 has a more dense layer stacking than in Mont-0, and the stacking remained substantially unchanged up to 673 K (MNC-4). Even in MNC-8, as can be seen from Fig. 4b, the layer stacking remained, even though it was dense. At 1273 K (MNC-10), stacking was destroyed resulting in the considerably homogeneous porous structure, i.e. pores of several μm in length and less than 1 μm in width orientated parallel to the film surface. Only the film surface becomes more dense, as well as in Mont-8.

TABLE III Identification of gases evolved from MNC by mass spectra*

HTT (K)	H_2O and/or NH_3	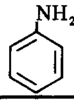	CO_2	CO
473–873	100	5	–	–
873–1473	13	–	9	100

*Numbers are relative intensity.

4. Discussion

On the basis of the above results, the thermal degradation processes of Mont and MNC are discussed.

4.1. Mont

X-ray diffraction and thermogravimetry indicate that Mont-10 loses absorped water below 473 K resulting in a basal spacing of 0.97 nm. Mont-2 used for FT-IR measurement, however, is rehydrated. In heat-treatment up to 673 K (Mont-4), the conversion of Mont to the amorphous phase occurs very slowly and then accelerates at 900 K at which point dehydroxylation starts. Such a conversion can be estimated from the strengthening of the background in contrast to the weakening of the diffraction peaks in the X-ray diffraction profile. In Mont-7 heated by 973 K, the resulting amorphous phase crystallizes slightly into LAS. Here the layer stacking is destroyed as can be seen from the SEM, but X-ray diffraction indicated remaining of a small amount of Mont crystal.

4.2. MNC

The hydrated Li^+ in Mont is replaced by NA to result in MNC. In view of the value of d_{001} of 0.96 nm of Mont after dehydration, the interlayer spacing of MNC-0 is expanded through insertion of NA by 0.73 nm. Elemental analysis of MNC-0 gives the chemical formula $C_{10}H_{15.3}N_{1.3}$ for the organic compound in MNC-0, which is very near to $C_{10}H_{10}N$ of NA. The difference in hydrogen content may be attributable to hydrogen from the montmorillonite structure. In addition, the chemical formula (Mont) $(NA)_{1.26}$ is deduced for MNC-0 from the elemental analysis of MNC-0.

After heating to 473 K, the carbon content somewhat decreased but infrared peak, attributable to C–N, NH_2 and C_{arom}–H, remained,

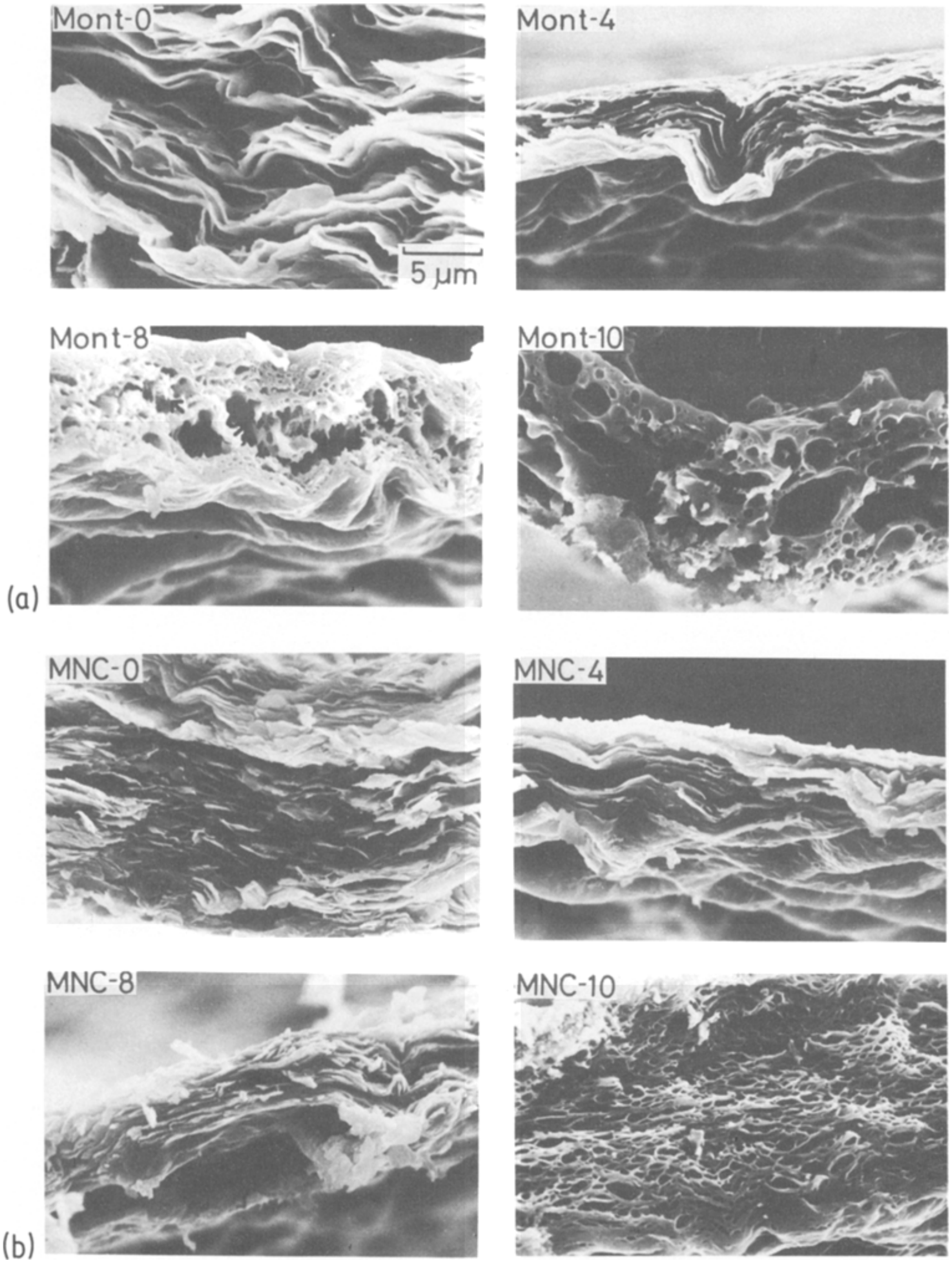

Figure 4 Scanning electron micrographs of (a) Mont and (b) MNC before and after heating.

i.e. NA remains substantially up to this temperature. It was impossible to obtain evidence for the polymerization of the inserted NA. However, irradiated MNC maintained its layered structure to a higher HTT than the unirradiated MNC, though not presented here.

Between 473 and 673 K, a large weight decrease was observed with remarkable decreases in carbon and nitrogen content and shrinkage of the interlayer spacing. NA is largely removed by this process. In view of the detection of aniline by mass spectrometry, NA may not be so seriously destroyed. A small amount of residue of aromatic structure, as shown by the infrared spectrum, acts to expand the interlayer spacing of montmorillonite by 0.29 nm.

At 673 to 873 K, the conversion of MNC into the amorphous phase proceeds as suggested from the strengthening of the background in the X-ray diffraction profile but the degradation mechanism is substantially similar to that of the previous process. Such changes are more accelerated at 873 to 1073 K. The following two phenomena are suggested to speculate the behaviour of the inserted residue, they are, (i) CO and CO_2 are the main gases evolved from MNC above 1073 K, and (ii) the carbon content decreases at this stage and increases again at 1473 K (MNC-12). Both phenomena suggest that the residue between the layers may be seriously destroyed and makes a strong bond with montmorillonite layer as explained later. In spite of such microscopic changes, the layer stacking is still maintained. It is also notable that MNC-8 exhibited a very sharp infrared absorption spectrum. This may be because an individual montmorillonite layer is favorably maintained by the inserted residue which was not destroyed, in spite of gradual changes of MNC into the amorphous as shown by X-ray diffraction.

At 1073 to 1273 K, the resulting amorphous phase changes into LAS and simultaneously, the layer stacking is also destroyed, as can be seen from Fig. 4b. One feature to be noted here is that treatment of MNC resulted in a homogeneous porous structure in which the elliptical pores aligned parallel to the film surface. This characteristic structure must result from the interference of sintering between the montmorillonite layers by the inserted residue and the evolved gases.

The crystallization of MNC proceeds further to result in cristobalite, mullite and cordierite crystals at higher HTT. Through such crystallization processes, the strongly bonded carbon atoms become separated, leading to an increase in carbon content in MNC-12 as shown in Table II.

Thus, the most interesting phenomena in the thermal degradation of MNC are (i) the thermal stability of the layered structure of montmorillonite which was improved remarkably through the insertion of NA, and (ii) the structure of MNC became homogeneous and porous after heating to 1273 K.

Acknowledgements

The authors wish to thank Professor M. Sato of Gunma University for his useful discussion and Mr A. Yoshida of The Musashi Institute of Technology for FT-IR measurement. Raw montmorillonite was kindly supplied by Kunimine Co. Ltd. The use of the Co-60 irradiation facility has been made possible by the Inter-University Program for the Common Use of JAERI Facilities.

References

1. M. S. WHITTINGHAM and R. R. CHIANELLI, *J. Chem. Ed.* 57 (1980) 569.
2. T. J. PINNAVAIA, *Science* 220 (1983) 365.
3. A. ŌYA, M. ŌTA and S. ŌTANI, *J. Mater. Sci.* 18 (1983) 1089.
4. A. ŌYA, K. YAMADA and S. ŌTANI, *ibid.* 17 (1982) 3617.
5. J. E. GRIESEKING, *Soil Sci.* 47 (1939) 1.
6. J. M. ADAMS and P. I. REID, *Clays Clay Miner.* 25 (1977) 228.
7. A. BLUMENSTEIN, *J. Polymer Sci. A* 3 (1965) 2665.
8. C. KATO, K. KURODA and M. MISAWA, *Clays Clay Miner.* 27 (1979) 129.
9. B. DURAND, R. PELLET and J. J. FRIPAIT, *ibid.* 20 (1972) 21.
10. A. ŌYA, F. TAMEGAI, M. SATO and S. ŌTANI, *J. Mater. Sci.* 16 (1981) 263.
11. M. SATO, private communication (1983).
12. V. STUBICAN and R. ROY, *Z. Krist.* 115 (1961) 200.
13. H. HAYASHI and K. OINUMA, *Clay Sci.* 1 (1963) 8.
14. TH. STUTZMANN and B. SIFFERT, *Clays Clay Miner.* 25 (1977) 392.

Received 27 February
and accepted 12 March 1984